Scientific Research Publishing

Journal of Geoscience and Environment Protection, 2022, 10, 121-135
https://www.scirp.org/journal/gep
ISSN Online: 2327-4344
ISSN Print: 2327-4336

Adsorption of Chromium (VI) Using Nano-ZnO Doped Scrap Tire-Derived Activated Carbon

Jean Tsitsi Chigova, Stanford Mudono

Department of Chemical Engineering, Faculty of Engineering, National University of Science and Technology (NUST), Bulawayo, Zimbabwe
Email: jeanchigova@gmail.com

How to cite this paper: Chigova, J. T., & Mudono, S. (2022). Adsorption of Chromium (VI) Using Nano-ZnO Doped Scrap Tire-Derived Activated Carbon. *Journal of Geoscience and Environment Protection, 10,* 121-135.
https://doi.org/10.4236/gep.2022.109008

Received: June 13, 2022
Accepted: September 24, 2022
Published: September 27, 2022

Abstract

Nowadays, nano mineral modified biochars show a promising adsorption capacity for pollutants removals by combining the advantages of porous structure of biochar and unique property of nano minerals. In this work, nano-zinc oxide doped scrap tire derived activated carbon (nZnO-STAC) was synthesized by wetness impregnation method. Equilibrium data were analyzed using Langmuir and Freundlich isotherm models while the kinetics of the process were examined using Lagergren Pseudo-first and second order, intra-particle diffusion and Elovich kinetic models. Characterization of the activated carbon by Powder X-ray Diffraction (PXRD). The surface groups present on the activated carbon surface were determined using the Fourier Transform Infra-Red Spectroscopy (FTIR) analysis. Optimization studies were carried out to determine the effects of pH, initial metal concentration, adsorbent dosage, contact time and adsorbent particle size on the Cr (VI) removal efficiency. The results showed optimum Cr (VI) removal at pH 3, 10 mg/L concentration, 120 minutes of contact using 1000 - 1400 μm adsorbent particle size at a dosage of 2.5 g/L. The adsorbent structure was found to be predominantly amorphous. The chromium removal efficiency of the adsorbent was around 81.6%. Of the tested kinetic models, the pseudo-second order model exhibited the best fit with the experimental data with an R^2 value of 0.9744. This study clearly demonstrates the feasibility of using the nano-ZnO doped scrap tyre derived activated carbon adsorbent for the remediation of chromium (VI) polluted industrial wastewaters.

Keywords

Adsorption, Zinc Oxide Nanoparticles, Tire Granules, Hexavalent Chromium, Tannery Effluent

1. Introduction

The presence of heavy metals in water bodies is a global environmental and ecological concern due to their non-biodegradability and persistence in the environment. Due to the non-degradable feature, phytoremediation and biosorption are two most often used methods to extract and enrich heavy metals by diverse plants from contaminated soil and water body (Singh et al., 2003). Heavy metals are present naturally in trace amounts but most of them including Arsenic, Lead, Cadmium, Nickel, Mercury, Chromium, Selenium, Cobalt and Zinc are very toxic even at low concentrations and cause deleterious effects to all spheres of the ecosystems (Jaishankar et al., 2014). They are introduced in large amounts through human activities such as mining, fossil fuel combustion, and overuse of agrochemicals, discharge of sewage sludge and various chemical processes (Hosney, 2015; Mella et al., 2016).

The leather tanning industry is one of the largest contributors of chromium pollution in the environment through leakages from process waters, chromium sludge from wastewater treatment, chrome-tanned leather shavings and chrome leather trimmings (Nigam et al., 2015). Hexavalent chromium, Cr (VI) is very toxic, carcinogenic, mutagenic to humans and animals and is associated with decreased plant growth and abnormalities in plant morphology (Oliveira, 2012). Chromium exists in many oxidation states ranging from −2 to +6, but the trivalent (+3) and hexavalent (+6) forms are prevalent in the environment (Nur-E-Alam et al., 2020). They are introduced in the environment through natural processes and anthropogenic activities, such as chromate production, chrome plating, leather tanning, dye and pigment manufacturing, textile dyeing and metal processing (Bielicka et al., 2005). These two chromium species have different biological, geochemical and toxicological properties. Trivalent chromium is less toxic whilst, hexavalent chromium is the most toxic form, with a reported toxicity of 500-times more than that of the trivalent one (Nur-E-Alam et al., 2020).

The high water solubility of Cr (VI) elevates the risk of this metal migrating to and contaminating groundwater bodies, leading to its entry into food chains and subsequent trophic transfer and biomagnification (Mangoma & Chigova, 2018). Cr (VI) is a particularly potent carcinogen at relatively low concentrations (parts per billion and parts per million) and is listed as a class A human carcinogen and as one of the 17 chemicals posing the greatest threat to humans by the United States Environmental Protection Agency (Bielicka et al., 2005). The World Health Organization (WHO) has established a threshold safety level of 50 mg of Cr (VI) per liter (Bielicka et al., 2005; Brymman, 2008). In aqueous solution, Cr (VI) hydrolyzes to $HCrO_4^-$, CrO_4^{2-}, and $Cr_2O_7^{2-}$ that are strong oxidants, moreover the Cr (VI) compounds are soluble and more mobile. The toxicity of Cr (VI) in humans has been linked to the chemical system resemblance between Cr oxyanions and sulfate ions (SO_4^{2-}) (Ammar et al., 2017; Chikobvu, 2020). Recent studies have shown that chromate compounds can induce DNA damage in various ways and can lead to the formation of DNA adducts, chromosomal aberra-

tions, sister chromatid exchanges, alterations in replication and transcription of DNA (Assem & Zhu, 2007; Jaishankar et al., 2014). In addition to these challenges, chromium ions and salts have also been shown to have toxic effects on the microbial consortia of wastewater treatment plants, thereby affecting their performance (Zahoor & Rehman, 2009). Wastewaters from industries like leather tanning, metal plating and paint and dye manufacture often contain high levels of chromium (VI) ranging from 2000 to 5000 mg/l (Belay, 2010). In order to avoid environmental deterioration, Cr (VI) must be reduced from the wastewater to recommended permissible discharge limits of 0.1 mg/L as stipulated by the Environmental Management Agency of Zimbabwe.

Several chromium removal techniques have been studied and employed such as chemical precipitation, reverse osmosis, ion exchange, coagulation, membrane filtration, adsorption and irradiation (Samantaray et al., 2014). These have certain limitations in their applications such as being expensive, time consuming, releasing additional waste to the environment and inability to remove heavy metals at very low concentrations (Brymman, 2008). However, adsorption is the most superior over some of the used techniques in wastewater treatment for the removal of heavy metal ions due to its simplicity, regeneration ability, cost-effectiveness, and also enabling largescale uses and ability to target a wide variety of contaminants and excellent removal efficiency (Dimpe et al., 2017; Gottipati, 2012; Silva et al., 2010).

Recent studies have highlighted that scrap tire granules can be activated using very low temperatures and used directly as a sorbent for the removal of heavy metals from aqueous solution. Ammar et al. (2017) showed that commercially activated carbons impregnated with copper oxide, zinc oxide and nickel oxide nanoparticles have higher adsorption efficiencies in the removal of sulfur from gasoil. Zinc oxide nanoparticles if well synthesized can be used efficiently in different applications, including wastewater treatment due to their non-toxicity, thermal stability, photocatalytic and antibacterial properties (Cruz, 2017). There is limited research and information available on the adsorption of Cr (VI) using nano-zinc oxide (nZnO)-doped waste tire derived activated carbon. This study seeks to assess the potential use of (nZnO)-doped activated carbon derived from waste tire rubber as a cheap adsorbent for the remediation of chromium-laden tannery effluent. In this way, a double benefit would be obtained as waste tire management is improved whilst also giving economic value to waste as a cheap raw material for making adsorbents.

In this study, tire granules will be activated by $ZnCl_2$ and calcined at a low temperature of 250˚C. Zinc oxide nanoparticles will then be doped into the waste tire derived activated carbon by the wetness impregnation synthesis method as described in the literature (Ammar et al., 2017). This will allow for the formation of a composite material with synergetic features such as high surface area, mechanical strength, thermostability and insolubility, antibacterial capacity and photocatalytic properties thereby enhancing hexavalent chromium removal from aqueous solution. The study will focus on the influence of various process

variables such as contact time, adsorbent dosage, adsorbent particle size and pH of the aqueous solution on chromium (VI) adsorption.

2. Materials and Method

2.1. Sample Preparation

The scrap tire sample was picked up at a local dumpsite and a composite effluent sample was collected from the aeration tank, sludge and wastewater treatment plant at Zambezi Tanners (Pvt) Ltd, Bulawayo, Zimbabwe. National University of Science and Technology (NUST) laboratory provided with analytical grade chemicals. Scrap tire was washed thoroughly using a detergent and tap water to remove dirt, rinsed with distilled water and left to air dry. The tire sidewalls, free of treads and steel breeds were cut into small granules using a scissors. To obtain smaller particle sizes ranging from 355 to 63 microns, an electric grinder was used. The scrap tire granules (STGs) were chemically activated by immersing 100 g of dried STG in 10% w/v zinc chloride ($ZnCl_2$) solution for 24 hours. The resulting product was kept in an air free oven maintained at 100˚C for 2 hours and then put in a muffle furnace for 1 hour at 250˚C, followed by washing with hydrochloric acid at a ratio of 1:1 to remove residual zinc chloride and further washed with distilled water to remove residual acid and zinc chloride until the water reached pH 7. The wet activated material was dried at 105˚C in an oven for 3 hours and stored in sealed air tight containers.

2.2. Impregnation of ZnO Nanoparticles onto STG Activated Carbon

Incipient wetness impregnation method was used to deposit the nanoparticles precursor zinc nitrate, ($Zn(NO_3)_2{\cdot}6H_2O$)) onto the activated STG using the method described by (Ammar et al., 2017) with minor alterations. The activated STGs were soaked in 10% w/w Zinc nitrate, solution for 24 hours at ambient conditions on an electric shaker (IKA KS 130 basic) at 160 rpm to load the largest amount of the metal precursor. The final product was filtered and dried in an air free oven at 90˚C for 6 hours and finally calcined in the furnace at a temperature of 250˚C for 3 hours to obtain ZnO nanoparticles.

2.3. Characterisation of the Adsorbent Using Powder X-Ray Diffraction (PXRD)

Powder X-ray diffraction (PXRD) measurements and Fourier Transform Infrared Spectroscopy (FTIR) analysis were used to characterize the synthesized nanocomposites. PXRD was performed on a Bruker D2 Phaser 2nd Gen diffractometer using Cu Kα-radiation (voltage = 30 kV, current = 10 mA, λ = 1.54184 Å) at 298 K was used to characterize the purity and phase of the nano-synthesized material (nZnO-STAC). The samples were then placed onto a zero-background sample holder and scanned over 2θ range 5˚ to 90˚ with a step of 0.35˚ increments. X-rays were generated with a current flow of 10 mA and voltage of 30 kV.

The FTIR analysis of the synthesized nanocomposites samples was recorded in the range 400 to 4000 cm^{-1} on Nicolet 6700 Thermo-Scientific Fourier Transform Infrared spectrophotometer. A small amount of sample was finely ground and mixed with KBr at a sorbent/KBr mole ratio of 1:10 and mounted on the spectrophotometer for data collection.

2.4. Preparation of Standard Solutions

A stock solution of 1000 mg/L of Cr (VI) was prepared by dissolving 2.829 g of potassium dichromate in 1 L of distilled water. Standard solutions ranging from 0 - 50 mg/L were prepared by diluting the stock solution and assayed using the Diphenyl carbazide (DPC) method as described by Ilias et al. (2011). The assay was carried out as follows: 100 µl of each standard solution was added to 10 ml of distilled water in a test tube, followed by the addition of 1 ml of diphenyl carbazide solution (prepared by dissolving 0.25 g diphenyl carbazide in 100 ml acetone and adding 1 drop of phosphoric acid). After careful mixing, the mixture was kept at room temperature for 10 minutes to allow for colour development, followed by measurement of absorbance at 540 nm. The results were used to plot a standard curve and the amount of residual hexavalent chromium in the supernatants were then estimated by extrapolation from the standard curve.

2.5. Adsorption Studies

The n-ZnO-doped scrap tire derived activated carbon (n-ZnO-STAC) adsorbent was investigated for its ability to reduce Cr (VI) under varying conditions. Batch adsorption tests were carried out at the desired pH values, Cr (VI) concentrations, n-ZnO-STAC dosage levels, n-ZnO-STAC particle size and contact time, in beakers containing a constant volume of Cr (VI) solution (50 ml) using a mechanical shaker at a constant agitation speed of 160 rpm. The same conditions were applied for the n-ZnO-doped commercial activated carbon (n-ZnO-CAC). After the adsorption experiments, the residual of Cr (VI) was determined by a UV-Vis spectrophotometer (Microprocessor UV-VIS single beam spectrophotometer L1-285, Lasany).

2.5.1. Effect of Particle Size

Both adsorbent samples were sieved using an electronic sieve shaker (Model ES200 Mark IV) and different particle sizes were obtained. The particle sizes obtained for n-ZnO-STAC were <355, 355 - 710, 1000 - 1400, 1700 and 2000 µm whilst those for n-ZnO-CAC were 355, 710 and 1000 µm. In a stoppered reagent bottle, 1g of adsorbent was added to 50 ml of sample with an initial Cr (VI) concentration of 50 mg/L and agitated at 160 rpm for 60 minutes using a mechanical shaker. The particle size was varied from 355 - 2000 µm for n-ZnO-STAC and 355 - 1000 µm for n-ZnO-CAC, keeping all other variables constant. After 60 minutes, the filtrate was obtained and analyzed for residual Cr (VI) concentration on the spectrometer. The particle size for optimum removal was obtained.

2.5.2. Effect of Concentration

To determine the effect of concentration on the adsorbent's Cr (VI) reducing abilities, 1 g of adsorbent (particle size 1000 - 1400 μm) was added to stoppered reagent bottles with 50 ml of sample with varying Cr (VI) concentrations from 10 - 50 mg/l. The mixture was agitated at 160 rpm for 60 minutes. The filtrate was analyzed for residual Cr (VI) concentration and the optimum concentration was obtained.

2.5.3. Effect of Contact Time

To determine the effect of contact time on Cr (VI) removal by the adsorbent, 1 g of adsorbent (particle size 1000 - 1400 μm) was added to the reagent bottle containing 50 ml of sample at a concentration of 50 mg/L and agitated at 160 rpm for different time intervals from 20 - 150 minutes. The solution was filtered and the filtrate analyzed for residual Cr (VI) using a spectrometer. The optimum contact time was obtained.

2.5.4. Effect of pH

In a stoppered reagent bottle containing 50 ml sample at 50 mg/L, 1g of adsorbent was added. The pH of the samples was then adjusted using 0.1 M NaOH and or 0.1 M HCl to pH 2 - 8. The reagent bottles were placed onto the mechanical shaker and agitated at 160 rpm for 60 minutes. The filtrate concentration was analyzed to get the optimum pH

2.5.5. Effect of Adsorbent Dosage

The effect of adsorbent dosage was determined by varying the adsorbent amount from 0.5, 1.0, 1.5, 2.0 and 2.5 g whilst holding all parameters constant. The filtrate was then analyzed for the residual Cr (VI) concentration to get the optimum.

3. Results and Discussion

3.1. Adsorbent Characterization

Instrumental techniques including Powder X-ray diffraction (PXRD) and FTIR spectroscopy have been employed to characterize the adsorbents used in this study.

3.1.1. XRD Analysis

X-ray diffraction was used to evaluate the crystal structure of the synthesized nanocomposites. The XRD spectra of the adsorbent are shown in **Figure 1** can be noted that nano zinc oxide scrap tire derived activated carbon is predominantly amorphous as shown by the presence of broad peaks and absence of sharp peaks, which is an advantageous property for well-defined porous adsorbents (Thangeeswari, George, & Kumar, 2017). The commercial activated carbon samples had sharp peaks characterizing the crystalline phase. Low intensity peaks were observed for nZnO-CAC sample hence it is not perfectly crystalline and this might be due to the modification of the adsorbent with ZnO nanoparticles.

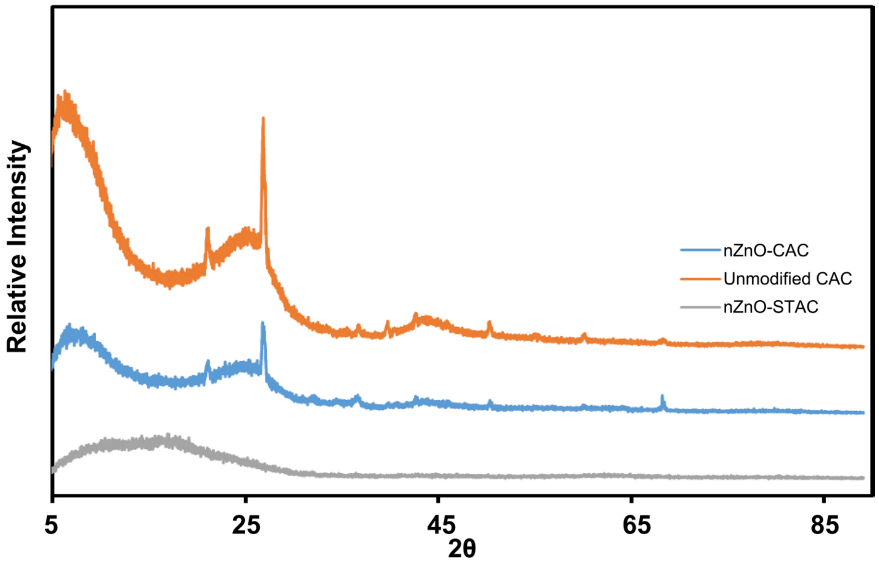

Figure 1. XRD spectra of unmodified CAC, nZnO-CAC and nZnO-STAC.

3.1.2. FTIR Analysis

FTIR spectroscopy was used to identify the functional groups on the surface of the functionalized synthesized nanocomposites, the chemical composition and quality of the adsorbents. The FTIR spectra of unmodified commercial activated carbon, nano doped commercial activated carbon and scraped tire derived activated carbon are presented in Figure 2. The spectra show that one major strong peak was observed at around 3400 cm^{-1} for the nZnO-CAC, nZnO-STAC and unmodified CAC, mainly attributed to the -OH group stretching due to the presence of water molecules. Peaks between 1500 - 2000 cm^{-1} suggest aromatic C=C ring stretching. The fingerprint of the samples is given by the peaks below 1500 cm^{-1}. Peaks around 1100 cm^{-1} are assigned to the C-C-C bending and those around 1330 - 1430 cm^{-1} are associated with O-H bending (in plane). The peaks ranging from 600 - 700 cm^{-1} are assigned to C-Br stretching halo-compound and C-H deformation. The C-Br peak was observed as a result of the bromine impurity introduced as KBr to the samples during pellet formation for the FTIR process. The peaks around 460 - 470 in nZnO-CAC and nZnO-STAC are associated with Zn-O stretching band evidencing that doping was successful in both adsorbents and the results are summarized in Table 1.

3.2. Effect of Particle Size

The effect of particle size on Cr (VI) uptake by the adsorbent was investigated. The batch adsorption of 50 mg/L Cr (VI) at initial pH value 5.6, contact time 60 minutes and a fixed adsorbent dosage of 1 g/L is shown in Figure 3. The trend observed indicates that an increase in particle size results in a decrease in the percentage Cr (VI) removed by the adsorbents. The Cr (VI) removal efficiency of nZnO-STAC decreased from 80.64% to 47.86% with increase in particle size from 355 to 2000 microns and from 94.95% to 84.31% with increase in particle size from 355 to 1000 microns for nZnO-CAC. This is consistent with literature

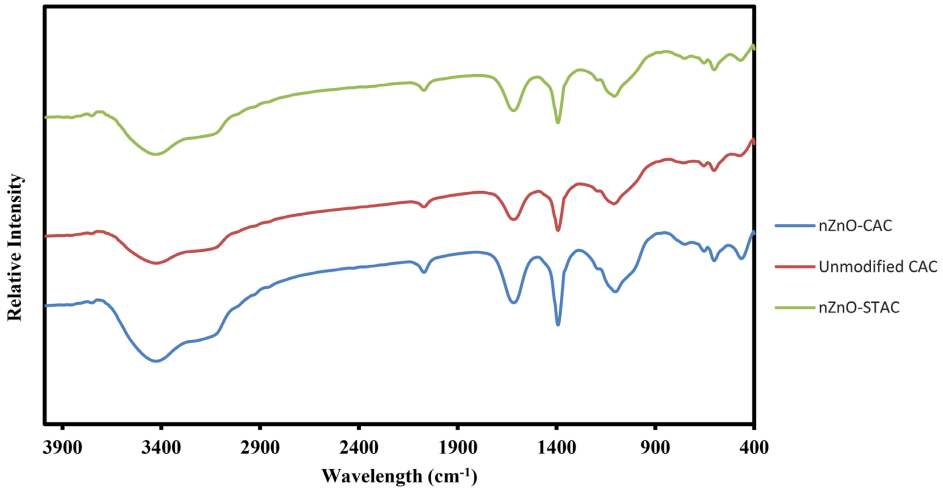

Figure 2. FTIR spectra of unmodified CAC, nZnO-CAC and nZnO-STAC.

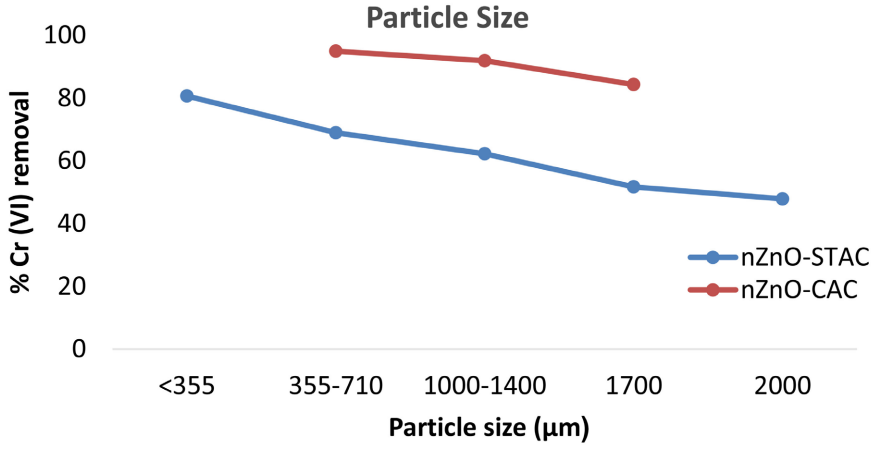

Figure 3. Effects of different adsorbent particle sizes.

Table 1. FTIR wave identification of unmodified CAC, nZnO-CAC and nZnO-STAC.

Wavelength (cm^{-1})	Unmodified CAC	nZnO-CAC	nZnO-STAC	Characteristic Vibration
3425 - 3429	Very strong	Very strong	Very strong	OH stretching (Al-Qodah & Shawabkah, 2009)
2070 - 2071	Medium	Medium	Medium	Aromatic C=C stretching N=C=S stretching (Özçimen & Ersoy Meriçboyu, 2010)
1617	Strong	Strong	Strong	Aromatic C=C stretching (Özçimen & Ersoy Meriçboyu, 2010)
1330 - 1430	Medium	Medium	Medium	Aldehyde OH bending (in plane) (Thangeeswari et al., 2017)
1100 - 1110	Medium	Medium	Medium	C-C-C bending Amine C-N stretching (Özçimen & Ersoy Meriçboyu, 2010)
602 - 605	Weak	Weak	Weak	Halo-compound C-Br stretching C-H deformation (Al-Qodah & Shawabkah, 2009)
464 - 468	No peak	Medium	Medium	ZnO stretching (Thangeeswari et al., 2017)

which states that the smaller the particle size sorbents are, the larger the surface area and consequently the greater the rate of diffusion and adsorption. Intra-particle diffusion is increased with an increase in particle size due to the longer mass transfer zone causing a slower rate of adsorption.

3.3. Effect of Concentration

Cr (VI) sorption was studied in batch experiments, pH 5.6, contact time 60 minutes and a constant adsorbent dosage of 1 g/L using different initial Cr (VI) concentrations of 10, 20, 30, 40 and 50 mg/L. The plot in Figure 4 shows that the overall percentage removal of Cr (VI) from solution decreases with an increase in initial Cr (VI) concentration from 10 - 50 mg/L. This may be due to the lack of sufficient active sites to accommodate much more metal available in the solution at high concentrations. As the initial metal concentration increases, the number of active sites on the adsorbent become limited as they saturate with the high ratio of Cr (VI) ions in solution. The percentage removal for an initial chromium concentration of 50 mg/L was 60.56% whilst that for an initial concentration of 10 and 30 mg/L was 78.62% and 64.05% respectively for nZnO-STAC. At an initial concentration of 50 mg/L, 83.70% Cr (VI) ions were removed whilst at 10 and 30 mg/L 100% and 90.31% was removed respectively for the nZnO-CAC sorbent.

3.4. Effect of Contact Time

According to Figure 5, the percentage removal of Cr (VI) increased from 37.82% to 69.28% for nZnO-STAC and 70.22% to 96.12% for nZnO-CAC with an increase in time from 20 - 150 minutes. The rate of adsorption was rapid within the first 60 minutes due to the availability of abundant adsorption sites on the adsorbent then became slower in the last 60 minutes due to mass transfer resistance and saturation of the adsorption sites. Furthermore, the diffusion of metal ions into the adsorbent pores will be occurring by the intraparticle diffusion mechanism. According to the results, the optimum time for the adsorption was

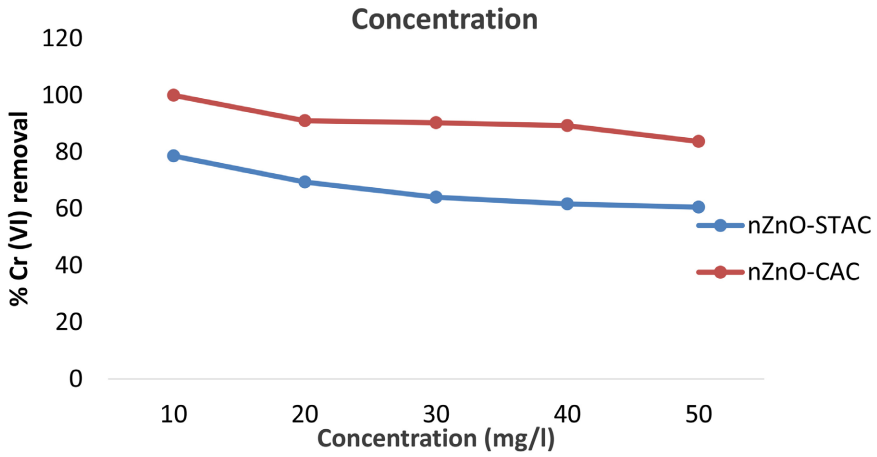

Figure 4. Effect of initial concentration on adsorption.

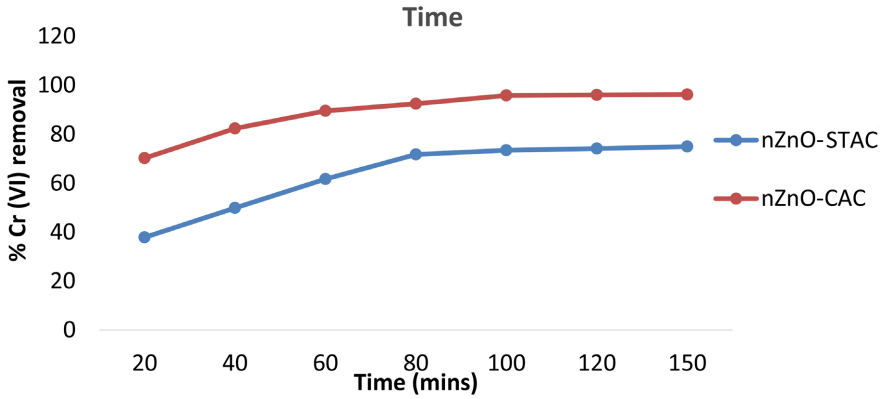

Figure 5. Effects of contact time on adsorption.

120 minutes, a further increase in contact time to 150 minutes did not bring about significant adsorption efficiency.

3.5. Effect of pH

In general, the removal of metal ions from an aqueous solution by adsorption is highly pH-dependent. This is due to the influence of pH on the surface charge as well as the degree of ionization and speciation of different pollutants (Mella et al., 2016). **Figure 6** shows that Cr (VI) removal efficiency increases at lower pH values and decreases at higher pH values. The maximum adsorption of Cr (VI) occurred in an acidic medium at pH 3.0 and after that the removal efficiency dropped significantly to 28.56% and 51.38% for nZnO-STAC and nZnO-CAC, respectively. In the pH range of 1.0 - 6.0, chromium ions co-exists in different forms such as $Cr_2O_7^{2-}$, $HCrO_4^-$, CrO_4^{2-} and H_2CrO_4. As the pH of the solution increases, the predominant chromium species are CrO_4^{2-} (dominant in pH range of 6.0 to 8.0). At higher pH values greater than 6.0, hydroxyl ions are predominant in solution and therefore compete with CrO_4^{2-} ions for the adsorption sites thus adsorption of chromium is decreased (Altia et al., 2010). More chromium adsorption at lower pH values is due to an increase in H^+ ions on the adsorbent surface at low pH which results in significantly strong electrostatic attraction between the positively charged adsorbent surface and the negatively charged $HCrO_4^-$ ions. Previous work on the adsorption of Cr (VI) ions from model chromium salt solutions using different adsorbents concluded that maximum adsorption efficiency is achieved in acidic mediums with pH of 2.5 - 4.0 (Mella et al., 2016).

3.6. Effect of Adsorbent Dosage

In order to assess the effects of the dosage amount, batch adsorption tests have been performed with different amounts ranging from 0.5 to 2.5 g/L while keeping other operating variables constant. It was noticed that by raising the adsorbent dosage, the Cr (VI) removal increases from 86.68% to 95.87%, for nZnO-CAC and 48.32% to 77.49% for nZnO-STAC as shown in **Figure 7**. An increase in

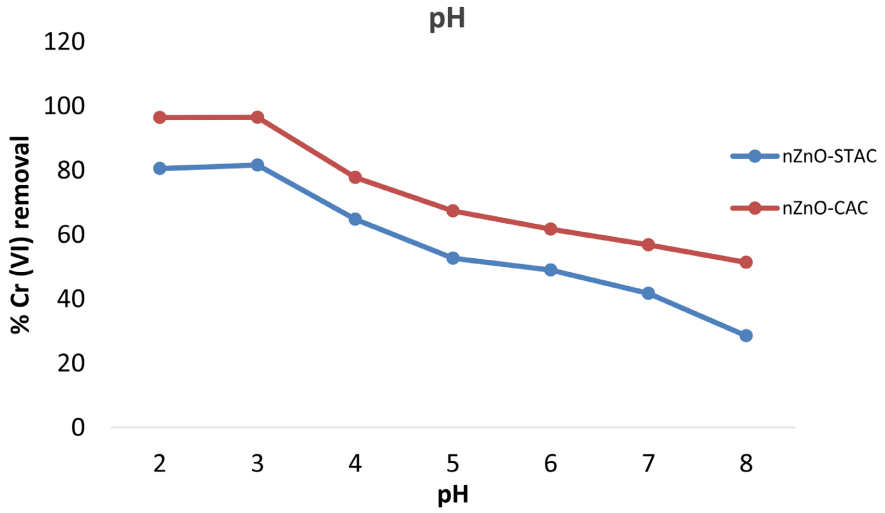

Figure 6. Effect of pH on adsorption.

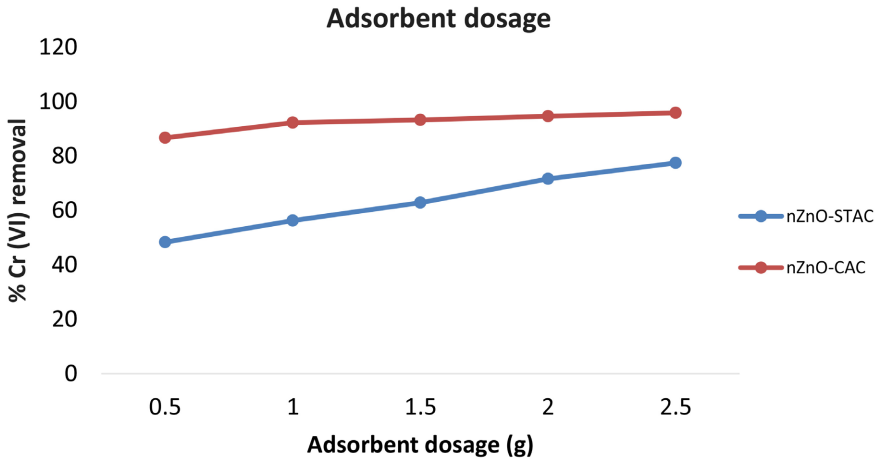

Figure 7. Effect adsorbent dosage.

adsorptive active sites leads to an increase the removal efficiency. Moreover, at a higher dosage of 0.30 g/L, Cr (VI) removal (%) stayed constant as a result of the adsorption equilibrium attainment. This is due to an increase in the number of available adsorption sites for chromium uptake hence the amount of Cr (VI) ions adsorbed increases. The results of this study also conforms to the results obtained by most researchers on the removal of Cr (VI) from aqueous solution by adsorption onto activated carbon (Hernández-peña et al., 2021).

3.7. Adsorption Isotherms

The equilibrium relationship between the amounts of Cr (VI) ions adsorbed and those in solution were determined using Langmuir adsorption isotherm model. Based on the Langmuir Isotherm model, uniform adsorption occurs on the active sites, and there is no more adsorption on these sites, once the sites are occupied with each site having the same binding energy (Venkatesham et al., 2013). Langmuir isotherm linear model is given by Equation (1):

$$\frac{Ce}{Qe} = \frac{1}{bQo} + \frac{Ce}{Qo} \quad (1)$$

where Qe (mg/g) is the adsorbed amount of Cr (VI), Ce (mg/L) is the equilibrium concentration of Cr (VI) in solution, Qo is the maximum sorption capacity (mg/g) of the adsorbent and b is the sorption constant (L/mg) at a given temperature. When the experimental data was fitted into the Langmuir equation, the values of b, R^2 *and* Qo were found to be 2.845, 0.9938 and 0.252 respectively for nZnO-STAC and 0, 1.0 and 1.0 respectively for nZnO-CAC and Figure 8 and Figure 9 show Langmuir isotherm models for nZnO-STAC and nZnO-CAC, respectively. From the values of the R^2 it can be seen that the synthesizes nanocompsite ZnO (0.9938) is similar to the commercial nanocomposite ZnO (1). The essential characteristics and feasibility of the Langmuir isotherm can be expressed in terms of a dimensionless constant separation factor, RL which is defined as:

$$RL = \frac{1}{1 + b \times Ci} \quad (2)$$

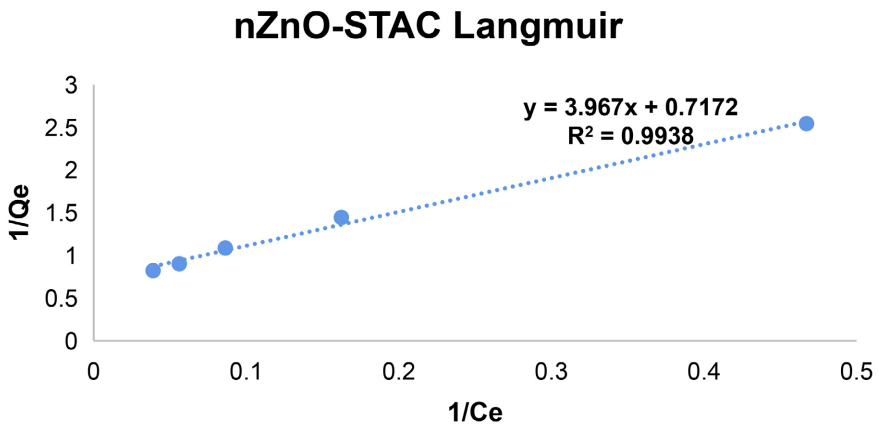

Figure 8. Langmuir isotherm for nZnO-STAC.

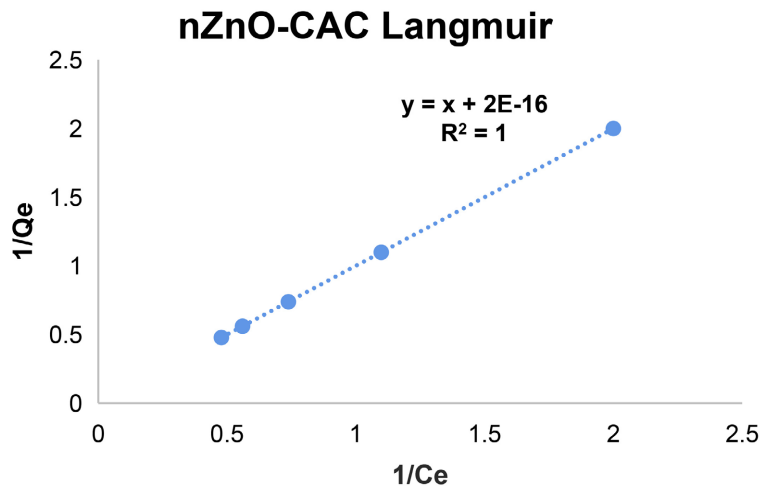

Figure 9. Langmuir isotherm for nZnO-CAC.

The isotherm adsorption data for the heavy metal were well fitted by Langmuir adsorption model suggesting the adsorbent surface contained identical sorption sites, and the sorption of adsorbate was monomolecular layer without interaction between the adsorbed molecules (Langmuir, 1918).

4. Conclusion

In summary, the adsorption capacity and removal efficiency using nZnO-STAC adsorbent synthesized by the wetness impregnation method were affected by pH, initial concentration, contact time, dosage amount, agitation speed, and the presence of competing anions. The Cr (VI) adsorption process followed the Langmuir adsorption model. The Langmuir monolayer adsorption capacity was 152.2 mg/g with Langmuir equilibrium constant of 3.204 L/mg at 298 K. The prepared activated carbon was successfully applied for the removal of Cr (VI) in effluent wastewater collected from a local tannery in Bulawayo and the optimum operating conditions for Cr (VI) adsorption were; pH 3.0, 120 minutes of contact, 2.5 g/L dosage and at a concentration of 10 mg/L. This study has revealed that a low cost nanocomposite adsorbent of nZnO-STAC synthesized by wet impregnation method can be used for removal of Cr (VI) from industrial effluents.

Acknowledgements

The research team thanks the National University of Science and Technology (Bulawayo, Zimbabwe), especially the departments of Chemical Engineering, Applied Chemistry and Applied Biology and Biochemistry for providing the resources and equipment for the success of the research. The research team also acknowledges and thanks Zambezi Tanners (Bulawayo) for the samples. Many thanks and gratitude goes to the Research Council of Zimbabwe (RCZ) for financial support.

Conflicts of Interest

The authors declare no conflicts of interest regarding the publication of this paper.

References

Al-Qodah, Z., & Shawabkah, R. (2009). Production and Characterization of Granular Activated Carbon from Activated Sludge. *Brazilian Journal of Chemical Engineering, 26,* 127-136. https://doi.org/10.1590/S0104-66322009000100012

Altia, B. et al. (2010). Adsorption of Chromium Ion (VI) by Acid Activated Carbon. *Brazilian Journal of Chemical Engineering, 27,* 183-193. https://doi.org/10.1590/S0104-66322010000100016

Ammar, S. H., Noryasmin, J., & Jaffa, S. A. (2017). Adsorptive Desulfurization of Gas Oil over Cu_2O/AC, ZnO/AC and NiO/AC Adsorbents. *Engineering and Technology Journal, 35,* 856-863. https://www.researchgate.net/publication/322445152

Assem, L., & Zhu, H. (2007). *Chromium Toxicological Overview* (pp. 1-14). Health Protection Agency, (III).

http://www.hpa.org.uk/webc/HPAwebFile/HPAweb_C/1194947362170

Belay, A. A. (2010). Impacts of Chromium from Tannery Effluent and Evaluation of Alternative Treatment Options. *Journal of Environmental Protection, 1,* 53-58. https://doi.org/10.4236/jep.2010.11007

Bielicka, A., Bojanowska, I., & Wiśniewski, A. (2005). Two Faces of Chromium—Pollutant and Bioelement. *Polish Journal of Environmental Studies, 14,* 5-10.

Brymman, A. (2008). *Preparation of Activated Carbon from Waste Tyres Char Impregnated with Potassium Hydroxide and Carbon Dioxide Gasification*. M.Sc. Thesis, University Sains.

Chikobvu, D. (2020). The Challenges of Solid Waste Disposal in Rapidly Urbanizing Cities: A Case of Highfields Suburb in Harare, Zimbabwe. *Journal of Sustainable Development in Africa, 13,* 184-199.

Cruz, G. J. F. (2017). Composites of ZnO Nanoparticles and Biomass Based Activated Carbon: Adsorption, Photocatalytic and Antibacterial Capacities. *Water Science and Technology, 2017,* 492-508. https://doi.org/10.2166/wst.2018.176

Dimpe, K. M., Ngila, J. C., & Nomngongo, P. N. (2017). Application of Waste Tyre-Based Activated Carbon for the Removal of Heavy Metals in Wastewater. *Cogent Engineering, 4,* Article ID: 1330912. https://doi.org/10.1080/23311916.2017.1330912

Gottipati, R. (2012). *Preparation and Characterization of Microporous Activated Carbon from Biomass and Its Application in the Removal of Chromium (VI) from Aqueous Phase* (pp. 1-242). Department of Chemical Engineering, National Institute of Technology.

Hernández-peña, C. C. et al. (2021). Reduction in Concentration of Chromium (VI) by *Lysinibacillus macroides* Isolated from Sediments of the Chapala Lake, Mexico. *Anais da Academia Brasileira de Ciências, 93,* e20190144. https://doi.org/10.1590/0001-3765202120190144

Hosney, H. (2015). *Preparation of Activated Carbon by Thermal Decomposition of Waste Tires for Pollution Control* (p. 34). Memoirs of the Faculty of Engineering, Minia University.

Jaishankar, M. et al. (2014). Toxicity, Mechanism and Health Effects of Some Heavy Metals. *Interdisciplinary Toxicology, 7,* 60-72. https://doi.org/10.2478/intox-2014-0009

Langmuir, I. (1918). The Adsorption of Gases on Plane Surface of Glass, Mica and Olatinum. *Journal of the American Chemical Society, 40,* 1361-1403. https://doi.org/10.1021/ja02242a004

Mangoma, N., & Chigova, J. T. (2018). Chromium (VI) Reduction by Bacteria Isolated from Tannery Effluent in Bulawayo, Zimbabwe. *African Journal of Microbiology Research*.

Mella, B., Glanert, A. C. C., & Gutterres, M. (2016). Removal of Chromium from Tanning Wastewater by Chemical Precipitation and Electrocoagulation. *Journal of the Society of Leather Technologists and Chemists, 100,* 55-61.

Nigam, H. et al. (2015). Effect of Chromium Generated by Solid Waste of Tannery and Microbial Degradation of Chromium to Reduce Its Toxicity: A Review. *Advances in Applied Science Research, 6,* 129-136. https://www.pelagiaresearchlibrary.com

Nur-E-Alam, M. et al. (2020). An Overview of Chromium Removal Techniques from Tannery Effluent. *Applied Water Science, 10,* Article No. 205. https://doi.org/10.1007/s13201-020-01286-0

Oliveira, H. (2012). Chromium as an Environmental Pollutant: Insights on Induced Plant Toxicity. *Journal of Botany, 2012,* Article ID: 375843.

https://doi.org/10.1155/2012/375843

Özçimen, D., & Ersoy-Meriçboyu, A. (2010). Characterization of Biochar and Bio-Oil Samples Obtained from Carbonization of Various Biomass Materials. *Renewable Energy, 35,* 1319-1324. https://doi.org/10.1016/j.renene.2009.11.042

Samantaray, D., Mohapatra, S., & Mishra, B. B. (2014). Microbial Bioremediation of Industrial Effluents. In S. Das (Ed.), *Microbial Biodegradation and Bioremediation* (pp. 325-339). Elsevier Inc. https://doi.org/10.1016/B978-0-12-800021-2.00014-5

Silva, H. S. et al. (2010). Adsorption of Mercury (II) from Liquid Solutions Using Modified Activated Carbons. *Materials Research, 13,* 129-134. https://doi.org/10.1590/S1516-14392010000200003

Singh, O. V., Labana, S., Pandey, G., Budhiraja, R., & Jain, R. K. (2003). Phytoremediation: An Overview of Metallic Ion Decontamination from Soil. *Applied Microbiology and Biotechnology, 61,* 405-412. https://doi.org/10.1007/s00253-003-1244-4

Thangeeswari, T., George, A. T., & Kumar, A. A. (2017). Optical Properties and FTIR Studies of Cobalt Doped ZnO Nanoparticles by Simple Solution Method. *Indian Journal of Science and Technology, 9,* 1-4. https://doi.org/10.17485/ijst/2016/v9i1/85776

Venkatesham, V. et al. (2013). Adsorption of Lead on Gel Combustion Derived Nano ZnO. *Procedia Engineering, 51,* 308-313. https://doi.org/10.1016/j.proeng.2013.01.041

Zahoor, A., & Rehman, A. (2009). Isolation of Cr (VI) Reducing Bacteria from Industrial Effluents and Their Potential Use in Bioremediation of Chromium Containing Wastewater. *Journal of Environmental Sciences, 21,* 814-820. https://doi.org/10.1016/S1001-0742(08)62346-3